# NOTICE

CERTAIN DATA CONTAINED IN THIS DOCUMENT MAY BE DIFFICULT TO READ IN MICROFICHE PRODUCTS.

CONF-9007136--4

LA-UR 90-3311

Los Alamos National Laboratory is operated by the University of California for the United States Department of Energy under contract W-7405-ENG-36

LA-UR--90-3311

DE91 000208

TITLE: CONCEPTS IN STRONG LANGMUIR TURBULENCE THEORY

AUTHOR(S): D. F. DuBois
Harvey A. Rose

SUBMITTED TO: Proceedings: Summer Institute in Theoretical Physics on Nonlinear and Chaotic Phenomena in Plasmas, Solids and Fluids, University of Alberta, Edmonton, Canada, July 16-27, 1990

## DISCLAIMER







Los Alamos National Laboratory
Los Alamos, New Mexico 87545



FORM NO. 836 R4
ST. NO. 2629 5/81

# CONCEPTS IN STRONG LANGMUIR TURBULENCE THEORY*

D. F. DuBois and Harvey A.Rose
Theoretical Division
University of California
Los Alamos National Laboratory
Los Alamos, NM 89545

## ABSTRACT

Some of the basic concepts of strong Langmuir turbulence (SLT) theory are reviewed. In SLT systems, a major fraction of the turbulent energy is carried by local, time-dependent, nonlinear excitations called cavitons. Modulational instability, localization of Langmuir fields by density fluctuations, caviton nucleation, collapse, and burnout and caviton correlations are reviewed. Recent experimental evidence will be presented for SLT phenomena in the interaction of powerful HF waves with the ionosphere and in laser-plasma interaction experiments.

## 1. Introduction

The study of Langmuir turbulence is usually defined as the study of the turbulent state generated by the interaction of high frequency electrostatic Langmuir (or electron plasma) waves and low frequency ion sound waves. The system is usually driven into the turbulent state by the interaction of these waves with high energy density beams of electromagnetic energy (e.g. lasers) or charged particles (e.g. electron beams). In recent years it has been increasingly realized that the approximation of weakly interacting, linear waves, as embodied in the so called weak turbulence theory (WTT), has a very limited domain of validity in describing the Langmuir turbulence driven by high energy density coherent external beams.

In the seminal work of Zakharov[1] in 1972 many of the basic concepts of strong Langmuir turbulence (SLT) theory were developed. Primary among these were special collapsing state solutions consisting of a high frequency Langmuir field

*This article is based on three lectures given by the authors at the Summer Institute in Theoretical Physics on Nonlinear and Chaotic Phenomena in Plasmas, Solids and Fluids, University of Alberta, Edmonton, Canada, July 16-27, 1990.

trapped in a self-consistent ion density depression which collapsed to a singularity in a finite time. We shall refer to such structures as cavitons. It was clear that if such solutions had a wide, and physically interesting, basin of attraction they would lead to an important source of dissipation of Langmuir energy. When the caviton's spatial dimensions collapse to a few electron Debye lengths, strong wave-particle damping occurs and energy is transferred from the electric field to accelerated electrons. This has now been well verified in experiment[2] and in particle-in-cell simulations[3] of isolated, undriven, collapsing cavitons.

Understanding of a truly turbulent, many caviton, state has been achieved using large spectral numerical simulation of the basic nonlinear "Zakharov" equations describing Langmuir turbulence.[4–12] These studies have shown that collapsing caviton states are indeed important and often the dominant attractors for a wide range of driving and initial conditions. In many cases a significant (sometimes dominant) fraction of the turbulent electric field energy is contained in collapsing cavitons. The simulation studies have also isolated the mechanisms through which energy is transferred from the external driving beams to the collapsing cavitons, which are usually the dominant dissipation sink. Although the details differ, depending on the driving source and parameter regime, a common element is that cavitons are *nucleated*[6] in preexisting ion density depressions. These preexisting ion density depressions are often the remnants of previous caviton collapse events. The nucleation concept has led to an increased awareness of the controlling influence that the ion density fluctuations have on determining the state of the Langmuir electric field. This has led, for example, to experimentally verified[13,14] predictions[15] of the nonlinear coupling of stimulated Raman scattering (SRS)-which excites Langmuir waves–to stimulated Brillouin scattering (SBS)–which excites ion density fluctuations (or ion sound waves).

The previous concept that the nonlinear state of SLT was sustained by repeated action of linear instabilities, such as the modulational instability, is not in agreement with the results of numerical simulation in many cases.

There are many linear instability mechanisms which can excite Langmuir waves from *quiescent* initial conditions and which evolve into states of SLT. These maybe used to define the physical domains in which SLT phenomena are important.

In the interaction of intense electromagnetic radiation with plasmas, the parametric decay instability[16,17] (PDI), the $2\omega_{pe}$ decay instability[18] and the SRS instability[19] can all excite Langmuir waves and the modulational[20] instability (MI) of the pump field can also drive up large Langmuir fluctuations. In short-wave-length, laser-plasma interactions the SRS and perhaps $2\omega_{pe}$ instabilities seem to be the most important. In ionospheric modification by powerful HF waves the MI and PDI play the dominant role. The latter experiments have been particularly fruitful in verifying some of the predictions of SLT theory.[21] A detailed discussion of SLT and its application to ionospheric heating phenomena near critical density is given in ref. 21 which we also refer to as I.

Intense charged particle beams can also excite various Langmuir wave instabilities. The electron bursts from solar flares are argued to excite SLT in

the solar wind plasma; the turbulent current fluctuations produce Type III radio emissions.[22,23] Laboratory experiments using nonrelativistic[2] and relativistic electron beams[24] may also excite SLT. The excitation of SLT by electron beams in the earth's electron foreshock has recently been studied.[25] Generally, we expect that states of SLT will be excited by any instability which strongly excites Langmuir waves in plasmas whose density gradients are sufficiently weak so that cavitons, accelerated in the gradient, move less than a typical caviton width before collapsing.

In this article we wish to review the basic concepts which are developing in our understanding of SLT. The approach will be highly heuristic and qualitative. A more complete list of references to work in this field can be found for example in references 21 (I), and 23. No attempt will be made here to give derivations.

## 2. Model equations for strong Langmuir turbulence

The most common model of SLT has become known as the "Zakharov model" although equivalent or closely related equations had been used previously by several other authors. Zakharov's seminal work[1] on collapse was the first to reveal the important nonlinear content of these equations.

The equations are a nonlinear set of PDE's coupling the envelope, $\underline{E}(\underline{x},t)$, $(\underline{\nabla}\times\underline{E})=0$, of the longitudinal Langmuir field to the fluctuation, $n(\underline{x},t)$, in the ion density. Quasi neutrality is assumed. In dimensionless form the equations are

$$\underline{\nabla}\cdot[i(\partial_t+\nu_e\bullet)+\nabla^2-n]\underline{E}=\underline{\nabla}\cdot\underline{S}_E(\underline{x},t) \tag{1}$$

and

$$(\partial_t^2+2\nu_i\bullet\partial_t-\nabla^2)n=\nabla^2|\underline{E}|^2+S_n(\underline{x},t) \tag{2}$$

The units are: time-$(3/2)\,\mathrm{M}\,\omega_p^{-1}$, space-$(3/2)\mathrm{M}^{1/2}\lambda_d$, electric field-$(4\pi n_o T_e)^{1/2}$ $(64\pi/3)(M/\eta)^{-1/2}$ and density-$(4/3)\ M^{-1}n_o$ where $M=\eta\ m_i/m_e$, $\eta$ is a constant of order 1, $n_o$ and $T_e$ are the background density and electron temperature, respectively.[21] The physical electric field is $R_e[\underline{E}(x,t)e^{-i\omega_p t}]$ where the carrier frequency is the mean plasma frequency $\omega_p$. As a further point of notation we adopt the following convention for spatial Fourier transforms: $\underline{E}(\underline{k})=(L)^{-D}\int d^Dx\ \exp\,[-i\underline{k}\cdot\underline{x}]\underline{E}(\underline{x})$ where D is the dimension of space.

The equations (1) and (2) are coupled through their nonlinear terms. The $-n\ \underline{E}$ term in (1) takes into account the density dependence of the electron plasma frequency; $\omega_p(n)=(4\pi\ e^2/m_e)^{1/2}(n_o+n)^{1/2}\simeq\omega_p(o)(1+n/2\ n_o)$ where $\omega_p(o)=\omega_p$ is the mean. The $\nabla^2|\underline{E}|^2$ term in (2) is the gradient of the low frequency ponderomotive force of the Langmuir field which tends to expell ion (and electron) density from high field regions.

To couple the collective fields, $\underline{E}$ and $n$ to the underlying discrete particle fluctuations damping operators $\nu_e \bullet$ and $\nu_i \bullet$, which are local in Fourier ($\underline{k}$) space but not in real space, have been included. The damping on the Langmuir waves $\nu_e$ can contain the effects of collisional and Landau damping. An ad hoc element of the theory, which is important to order to have well-resolved simulations, is that $\nu_e(k)$ must increase at least as fast as $k^{D/2}$, where D is the dimension of space, to prevent singular collapse for $D \geq 2$. It can be argued, as in I, that this type of damping models the nearly complete burnout of the E field observed in PIC simulations of collapse[3] and that many macroscopic properties of SLT, including the average energy dissipation rate, are not sensitive to the details of this damping.[21] In the simulation work reported here $\nu_i(k) = \nu_i|k|$ is used as a model of ion wave Landau damping. The source terms $\underline{S}_E$ and $S_n$ take into account the coupling to the external electromagnetic beams. [In principle $\underline{S}_E$ and $S_n$ also account for the particle noise related to the damping terms $\nu_e$ and $\nu_i$ so that (1) and (2) can be regarded as equations of the Langevin-type.] For systems driven by charged particle beams the usual approximation is to consider $\nu_e(k)$ to be *negative* over some domain of $\underline{k}$ to account for the particle-wave beam instability.[11,12,25]

A nice property of equations (1) and (2) is that they contain, when properly linearized, all the instabilities[15,21] (except $2\omega_{pe}$) referred to in Section 1. [Very similar equations apply to the $2\omega_{pe}$ case.]

In most of the specific examples which we will give here the sources will be those appropriate for the interactions of a spatially uniform pump field at a frequency $\tilde{\Omega}_o = \tilde{\omega}_o + \omega_p$ in physical units. In the envelope representation used in (1) we have

$$\underline{E}_o(t) = (\underline{E}_o e^{-i\omega_o t}) \tag{3}$$

where $\omega_o = (3/2)(\eta m_i/m_e)(\tilde{\omega}_o/\omega_p)$ in scaled units. In this case

$$\begin{aligned} \underline{S}_E &= n(\underline{x},t)\underline{E}_o e^{-i\omega_o t} \\ S_n &= \nabla^2[\underline{E}_o^* e^{i\omega_o t} \cdot \underline{E}(\underline{x},t) + \underline{E}_o e^{-i\omega_o t} \cdot \underline{E}^*(\underline{x},t)] \end{aligned} \tag{4}$$

We will refer to this type of driving as *parametric drive*. This drive is appropriate for electromagnetic drivers near the critical density ($\omega_o \sim 0$) such as in HF modification of the ionosphere.

## 3. Weak turbulence theory (WTT)

The approximation of WTT can be applied to (1) and (2) to obtain standard results. A basic assumption of WTT is that the power spectral densities $\langle|E(\underline{k},\omega)|^2\rangle$ and $\langle|n(\underline{k},\omega)|^2\rangle$ contain only the frequencies associated with free or linear Langmuir waves and ion acoustic waves, respectively:

$$\langle \underline{E}^*(\underline{k},\omega)\cdot\underline{E}(\underline{k}',\omega')\rangle = n_l(\underline{k})2\pi\delta(\omega-\omega_L(k))(2\pi)^{D+1}\delta(\omega-\omega')\delta^D(\underline{k}-\underline{k}^1)$$

$$\langle n^*(\underline{k},\omega)n(\underline{k}',\omega')\rangle = [n_S(\underline{k})2\pi\delta(\omega-\omega_S(k)+n_S(-\underline{k})2\pi\delta(\omega+\omega_S(-k)] \times(2\pi)^{D+1}\delta(\omega-\omega)\delta^D(\underline{k}-\underline{k}') \tag{5}$$

Here $\omega_L(k)=k^2$ which is the linear Langmuir wave frequency (relative to the envelope frequency $\omega_p$) and $\omega_S(k)=|\underline{k}|k*$ is the ion acoustic frequency ($k*=\sqrt{1-\nu_i^2}$ in our dimensionless units is also the ion sound speed).

WTT is basically a perturbation theory of linear waves based on the 3 wave interaction represented in Fig. 1. This interaction involves the familiar decay-type interactions with the frequency resonance conditions

$$\omega_L(\underline{k})=\omega_L(\underline{k}')\pm\omega_S(|\underline{k}-\underline{k}'|)\ . \tag{6}$$

The source term (4) also introduces the direct 'decay' of the pump

$$\omega_o=\omega_L(\underline{k})\pm\omega_S(-\underline{k}) \tag{7}$$

There are very many works on WTT. Here we refer to recent work[26] on the validity of WTT and in which references to other work can be found.

## III. Modulational instability and localization by density fluctuations

The concept of the modulational instability of extended Langmuir wave packets is well-known.[20] The mechanism is illustrated in Fig. 2. If a ripple is imposed on an otherwise nearly uniform Langmuir field (or on the driving field $\underline{E}_o$) the ponderomotive force associated with the peaks in $|\underline{E}(\underline{x},t)|^2$ tends to expell electrons and ions, causing density depressions in the high field regions. These density depressions tend to further confine (or trap) the E field increasing the sharpness of the peaks in $|E|^2$ further depleting the density and leading to an instability. Mainly from numerical simulation, we know that the nonlinear stage of this instability is an array of solitons in one dimension (D=1) and in D $\geq$ 2 an array of collapsing cavitons. The wavenumber of the dominant perturbation excited by the instability is $k_{MI}\sim W^{1/2}$ where $W=|\underline{E}|^2$ is the electric field

energy density of the original extended Langmuir wave. If the wavepacket is not uniform so that $|\underline{E}(\underline{k})|^2$ has a spectrum of width $\Delta k$ peaked say at $k = 0$, then there is a threshold[32] for modulational instability $W \gtrsim 2(\Delta k)^2$. Thus for a given value of the spatial averaged $W = \int d\underline{k}|E(k)|^2$, if $\Delta k \simeq k_{MI}$, i.e. if the spatial structure of $|E(x,t)|^2$ is on the same scale as $2\pi/k_{MI}$, the MI is suppressed. Generally, the spectrum of $\langle|E(k)|^2\rangle$ of the developed SLT state is so broad that the MI is suppressed.

Localized E fields can also arise through their coupling with ion density fluctuations n. From (1) we can find an eigenvalue equation[21] determining a complete orthonormal set of curl free vector eigenstates $\underline{e}_\nu(\underline{x},t)$ of the Langmuir field in a *given* ion density fluctuation profile $n(\underline{x},t)$

$$\underline{\nabla}\cdot(\lambda_\nu(t) + \nabla^2 - n(\underline{x},t))\underline{e}_\nu(\underline{x},t) = 0 \tag{8}$$

where

$$\underline{\nabla}\times\underline{e}_\nu = 0 \quad \text{and} \quad \int dx^D\ \underline{e}^*_\nu(x,t)\cdot\underline{e}_{\nu\prime}(xt) \equiv \langle e_\nu \mid e_{\nu\prime}\rangle = \delta_{\nu\nu\prime} \tag{9}$$

In D=1 this reduces to a familar Schrödinger equation in a "potential" $n(\underline{x},t)$. Depending on the profile of $n(\underline{x},t)$ the eigenstates $\underline{e}_\nu(\underline{x},t)$ may be localized in nature or extended. Plane wave solutions $\underline{e}_\nu = \hat{\underline{k}}\ e^{i\underline{k}\cdot\underline{x}}L^{-D/2}$ exist for $\lambda = k^2$ when $k^2 \gg |n|_{max}$, corresponding to free Langmuir waves. Since $n(\underline{x},t)$ is generally a function of time we have a different set of $\underline{e}_\nu(\underline{x},t)$ at each t which are continuously related. [In a finite box with a countable number of states the Hilbert space has the same dimension for all t.]

In general it is difficult to characterize the properties of this complete set of states. In one dimension (D=1) the eigenstates can be computed quite easily[6] for a given realization of $n(x,t)$. The states with the lowest (negative) eigenfrequencies $\lambda_\nu$ correspond to eigenfunctions which are mainly localized on density depressions. The localization of most interest here is on the scale of a single density depression not the more global localization of states, say, on the scale of the correlation lengths associated with random potentials. The short scale localization produces a ponderomotive force which may lead to collapse. The deep density depression where $\lambda_\nu \ll 0$, of the collapsing caviton produces a very localized or truly bound state.

We can specify these states for simple, idealized cases such as an isolated caviton at x=0. For $\lambda_\nu < 0$ we have truly bound states which for example in D=1 die as exp $-|\lambda_\nu|^{1/2}|\underline{x}|$ as $x \to \infty$; for $\lambda_\nu > 0$ we have extended or nearly free Langmuir waves (for $\lambda_k \simeq k^2 > n_{max}$). In section 5 we will generalize the concept of localized states to include long-lived metastable states with $n_{max} > \lambda_\nu > 0$. The condition for true bound states or for long-lived metastable states to exist is that $|n_{min}|\delta^2 \gtrsim 0(1)$ where $n_{min} < 0$ is the depth of the density well and $\delta$ is its spatial width.

Formally we may expand $\underline{E}(\underline{x},t)$ in this complete set of states

$$\underline{E}(\underline{x},t) = \sum_{\nu} h_{\nu}(t)\underline{e}_{\nu}(\underline{x},t) \tag{10}$$

In the case $\omega_o \lesssim 0$ the states in this sum can be divided into localized and extended so that $\underline{E}$ can be represented as the sum of a localized and extended part (see I). In other cases $\underline{E}$ has the same two component form but the use of the eigenstate expansion is not useful. An alternative approach is discussed in Section 7. The density wells which trap these localized states might arise from initial background density fluctuations, from density wells remaining from earlier collapse events or from density fluctuations driven by some instability such as SBS.

In the case of SBS-generated ion sound waves, we can sometimes regard these density fluctuations as being periodic in space with a wavelength corresponding to the fastest growing SBS mode. The eigenstates $\underline{e}_{\nu}(x,t)$ in this case can be regarded as one dimensional Bloch waves in a periodic potential, with lattice wave vector $\underline{k}$ and with eigenvalues $\lambda_{\underline{k},\nu}(t)$ which lie in bands, labelled by the index $\nu$, just as in solid state physics.[15] As the periodic density fluctuation grows exponentially in time due to the SBS instability the Langmuir mode eigenfrequencies $\lambda_{\nu k}(t)$ change in time. If a stimu' 'ted Raman instability is simultaneously excited, the SRS frequency matching condition, $\Delta\omega = \omega^{laser}_{\underline{k}_o} - \lambda_{\underline{k},\nu}(t) - \omega^{scatteredlight}_{\underline{k}_o - k} = 0$, can only be satisfied instantaneously for a given Langmuir Bloch mode with lattice wave vector $\underline{k}$. In fact if $\left|\frac{d\Delta\omega}{dt}\right| = \left|\frac{d}{dt}\lambda_{k,\nu}\right| > \gamma_R^2$, where $\gamma_R$ is the instantaneous SRS growth rate, then it can be shown[15] that the SRS instability is *detuned* by the growing SBS ion sound wave and SRS is suppressed. Experiments carried out at the NRC Laboratory in Canada[13,14] appear to be consistent with this scenario. The experiment by Villeneuve et al.[14] verified the theoretical prediction[15] that a "seeded" SBS instability could suppress SRS. In other parameter regimes where SRS is not suppressed the (weaker) SBS ion sound wave may still impose its spatial periodicity on the SRS Langmuir eigenfunctions.[15] These envelope eigenfunctions have a periodic array of maxima of $|\underline{E}|^2$ (or $|\underline{e}_{k,\nu}|^2$) which have a finite ponderomotive force (PMF). This periodic PMF causes a periodic array of density wells to develop in which the Langmuir waves are trapped and can be driven to collapse. [Note the ponderomotively driven periodic density wells do not coincide in general with the density minima of the SBS sound waves but they have the same periodicity.] In Fig. 3 taken from ref. 15, we show typical spatial configurations of $|E|^2$ and n, before and after collapse and burnout.

The impulsive time signature of the Thomson-scattering signal from Langmuir fluctuations in the experiment of Walsh et al.,[13] is consistent with the collapse of SRS driven Langmuir fluctuations. The large ion density fluctuations remaining from the burntout cavitons then act as seeds for the subsequent strong SBS pulse. In Fig. 3 the time signatures of the Langmuir and ion sound fluctuations, obtained from numerical solutions of the SRS-SBS driven Zakharov

equations, are shown. Further evidence consistent with the controlling effect of SBS generated ion sound waves on the SRS process is found in the experiments of Baldis et al.[27]

## 5. Langmuir collapse of cavitons

In 1972 Zakharov introduced the concept of Langmuir collapse.[1] He showed that for D $\geq$ 2 the ponderomotive pressure can overcome the thermal pressure (the $\nabla^2$n term) in (2) leading to collapsing solutions which reach singularities in a finite time (without dissipation). These collapsing solutions are localized states and have self-similar asymptotic forms.

$$\underline{E}(\underline{x},t) = \frac{1}{\delta(t)^{D/2}}\,\underline{\varepsilon}\left(\frac{\underline{x}}{\delta(t)}\right)\,\exp\,-i\int_o^t dt\lambda(t) \tag{10}$$

and

$$n(\underline{x},t) \;=\; \frac{1}{\delta^2(t)}\,\hat{n}\,\left(\frac{\underline{x}}{\delta(t)}\right) \tag{11}$$

where for supersonic collapse

$$\delta(t) = (t_c - t)^{2/D} \tag{12}$$

and $\lambda(t) \sim \delta(t)^{-2}$. Here $t_c$ is the time of collapse.

This solution conserves an invariant of (1) and (2) (in the absence of dissipation) which is the electrostatic energy in the caviton

$$N \;=\; \int d^D_{\underline{x}}|E(\underline{x},t)|^2 \;=\; \int d^D\xi|\underline{\varepsilon}(\underline{\xi}|^2 \tag{13}$$

In two dimensions, for the scalar form of Zakharov's equations in D=2, it is known[28] that *at least* a critical amount, $N_c$, of electrostatic energy must be carried into collapse where $N_c \simeq 10$ in our units. For the full vector equations (1) nothing to known rigorously but empirically we find $N_c \sim 50$. In D=3 collapse is possible for any value of N.

It is generally found[3,8,10] that the *shape* of the collapsing solution, as determined by $|\underline{\varepsilon}(\underline{x}/\delta(t)|^2$ and $\hat{n}(\underline{x}/\delta(t))$, has a "pancake" shape with the ratio of the thin dimension to the thick (radial) dimension in the range of 1:2 to 1:3. In the case of parametric pump drive the axis of the pancake, along the thin dimension, tends to be along the direction of $\underline{E}_o$. (At least in the case where there is direct nucleation by the pump as discussed in Section 5.)

The bound state eigenfunctions $\underline{e}_\nu(\underline{x},t)$ associated with collapse have this self-similar form except that they are normalized to carry a unit of energy i.e. $\int d^D\xi |\underline{e}_\nu(\underline{\xi})|^2 = 1$. Such a state is excited with an amplitude $h_\nu(t)$ such that the contribution to $\underline{E}(x,t)$ is $h_\nu(t)\underline{e}_\nu(x,t)$ and the energy carried into collapse is then $N = |h_\nu(t)|^2$.

The energy taken into collapse maybe gathered by the evolution of a modulational instability (MI) or by the transfer of energy from the driving source to the localized Langmuir states[29] in the nucleation process discussed in the next section.

## 6. Nucleation of localized caviton states and caviton cycles

How does the energy from the external driving sources communicate with the cavitons which dissipate most of the energy? A rather detailed understanding[6–9,21] has been gained for the case of parametric drive where $\omega_o < n_{max}$ where $n_{max}$ is defined below. This includes the case of overdense drive, $\omega_o < 0$, when the pump frequency is slightly less than the drive frequency.[21] In this case the parametric pump directly couples to the localized states of the cavitons. For $\omega_o \gg n_{max}$ and for beam drive[12] it appears that the long wavelength, free Langmuir waves, which are driven by coupling to the drive, couple to the localized states in the nucleation process. This indirect nucleation case is less well understood on the microscopic level.

An equation of motion for the amplitudes $h_\nu(t)$ can be obtained by the substitution of (10) into (1) using the source in (4). The complete result is given elsewhere.[21] If the coupling between a given localized state $\underline{e}_o(\underline{x},t)$ and all other states and damping is ignored the equation of motion for $h_o(t)$ is[21]

$$i\,\dot{h}_o(t) - \lambda_o(t)h_o(t) \;=\; \underline{E}_o \cdot \int d^D x\; \underline{e}_o^*(\underline{x},t)\; n(\underline{x},t)\;. \qquad (14)$$

Which has the form of a driven oscillator which has a time dependent (or chirped) frequency $\lambda_o(t)$. To use this equation $n(\underline{x},t)$ must be determined, say, from a simulation of the complete turbulent system. We have been able to carry out this program in one dimensional models where it is relatively easy to compute all of the $\lambda_\nu$'s and $e_\nu$'s. In this case (14) represents very well the evolution of a localized state as it gathers energy and begins to collapse.[6,7] In Fig. 4 we show results for the evolution of a localized state for the case of the scalar Zakharov equations where the density perturbation $n$ is taken to have radial symmetry $n = n(r,t)$ in 3 dimensions. This scalar model has the same collapse scaling exponents as the 3D vector Zakharov equation and also has the common property that a bound (or localized) state can be lost as the density well expands which results in a finite nucleation threshold for $E_o$. In Fig. 4a the dashed line shows the relaxation of the density well, $n(r=0,t)$, beginning from a deep negative value and relaxing to a small negative value before suddenly dropping to very

negative values corresponding to collapse. The density fluctuation is driven by the ponderomotive force, $|h_o(t)|^2\nabla^2|e_o(r,t)|^2$, of this single localized state and the case of strong ion damping $\nu_i \gtrsim 0.6$ is taken so that the density well does not bifurcate significantly following the burnout of the electric field. The solid line shows the corresponding $|E(r=0,t)|^2$ which suddenly peaks during collapse. The subsequent sudden drop is the burnout process in which the Langmuir energy is dissipated by wave-particle damping. In Fig. 4b the solid line shows the evolution of the localized state eigenvalue, $\lambda_o(t)$, which evolves from very negative values (since the state is originally deeply bound in a deep well) to a smaller negative value. [The dashed line shows the evolution of the time derivative of the phase $\Phi_o$ where $h_o(t) = |h_o(t)|\exp i\Phi_o(t)$; see I for a more complete discussion.] In this case the drive frequency is at $\omega_o = 0$. As the eigenvalue $\lambda_o(t)$ approaches the pump frequency the energy $|h_o(t)|^2$ (Fig. 4c) in the localized state increases rapidly as the mode frequency comes into closer resonance with the pump frequency ($\omega_o = 0$). This rapidly increases the PMF associated with the localized state, and as the density well deepens again in response to this PMF, $\lambda_o(t)$ again decreases rapidly during collapse.

A number of scaling laws for the dependence of various caviton parameters on the pump strength $E_o$ have been deduced from these isolated caviton studies.[21] For example, the peak value of $|E(r,t)|^2$ in the caviton at collapse scales as $E_o^{-2}$; the peak field in the caviton actually decreases with increasing driving strength.

The discussion above strictly only applies for $\omega_o \lesssim 0$, for sufficiently strong $E_o$, where the eigenvalue satisfies $\lambda_o(t) \leq \lambda_{max} < 0$. In this case the state at any time t, $\underline{e}_o$ is a true bound state whose amplitude is exponentially small as $|\underline{x}| \to \infty$. However, we know from simulations that a similar scenario applies for a range of $\omega_o > 0$. In this case the near resonance condition, $\lambda_o(t) \simeq \omega_o$ can imply $\lambda_o(t) > 0$ during the nucleation phase and such a state cannot be a true bound state. [During the collapse phase $\lambda_o(t) \ll 0$ and the state is a true bound state.] This case can be understood in terms of metastable states (or resonance scattering states) which occur in quantum mechanics (and elsewhere) in the well-known problem of a potential well surrounded by a potential barrier. [A good reference is D. Bohm, "Quantum Theory," Prentice Hall, 1952]. In the problem at hand a one dimensional example illustrates what we believe are the important points: Consider a density fluctuation profile, $n(\underline{x},t)$ (our "potential"), consisting of a potential well at $x = 0$ and a maximum (or barrier) at $x = \delta$ where $n(x=\delta,t) = n_{max}(t)$. For simplicity take $n(x) = n(-x)$. It is well known that localized metastable states can be constructed in the well which have all the properties of bound states except that they may have a finite lifetime, $\Delta t_N$, due to the leakage of the wavefuntion through the barrier. In the WKB approximation the lifetime of this state can be written as

$$\Delta t_N = \tau_o \exp[2\int_{x_N}^{x_b} dx(n(x,t) - \lambda_N(t))^{1/2}] \tag{15}$$

where $\tau_o = 2\int_o^{x_N} dx(\lambda_N - n)^{-1/2}$ is the time (in the WKB approximation) for a trapped Langmuir wave (packet) to cross the well and back. In (15), $x_N(t)$ is

the classical turning point *inside* the well where $n(x_N, t) = \lambda_N(t)$ and $x_b$ is the turning point (if any) outside of the barrier. [In the WKB approximation the eigenvalue, $\lambda_N$, is determined by the Born-Sommerfeld quantization condition, $2\int_o^{x_N} dx\sqrt{\lambda_N - n} = (N + 1/2)$, where N is an integer. The general form of $\Delta t$ may be valid for a thick barrier even if the WKB quantization condition is not.] The nucleation picture discussed above applies to the metastable states so long as their lifetime is long compared to other times of interest. For example near the maximum of $\lambda_o(t_o) = \lambda_{max}$, where $d\lambda_o(t_o)/dt = 0$, if $(\Delta t_N)^{-1} < (d^2\lambda_o/dt^2)^{1/3}_{t=t_o}$ the lifetime of the metastable state will not strongly effect the direct nucleation by the pump as calculated from (14).

For an isolated collapse with sufficiently strong ion sound damping the ion density profile of the evolving burntout cavity has the well-plus-barrier form where $n_{min} < 0$ and $n_{max} > 0$ and where the positive and negative regions are such as to conserve particle number: $\int d\underline{x} n(\underline{x}, t) = 0$. In this case for $\omega_o \leq 0, \lambda_{max} < 0$ for sufficiently strong $E_o$. the outside turning point is at $x_b = \infty$ and $\Delta t = \infty$, characteristic of a true bound state. For $0 < \lambda_{max} \lesssim \omega_o, \Delta t$ can still be large if $\lambda_{max} \lesssim \omega_o \ll n_{max}$.

This illustrates what we believe to be the typical nucleation behavior in this regime of direct coupling of cavitons to the pump: As the relaxing density well becomes shallower and broader its eigenvalue approaches resonance with the pump causing a rapidly increasing PMF which initiates the next collapse.

For isolated cavitons this behavior can evolve into a strict limit cycle of repeated nucleation-collapse-burnout. (The minimum value of $E_o$ which can sustain collapse at a given site is the nucleation threshold referred to above.) For overdense drive, $\omega_o < 0$, we have found limit cycle behavior even in the multicaviton case. In such regimes neighboring caviton's cycles are either in phase or $\pi$ out of phase. (The phase is defined as $2\pi\Delta t/\tau_c$ where $\tau_c$ is the cycle period and $\Delta t$ the collapse time modulo $\tau_c$.) Caviton correlations are discussed in some detail in Section 8.

A numerical diagnostic of how the pump energy is injected into the system is the injection spectrum $I_J(k) \equiv Im\langle \underline{E}_o \cdot \underline{E}^*(\underline{k}) n(-\underline{k})\rangle$. For parametric drive with $\omega_o \simeq 0, I_J(k)$ is a relatively broad spectrum extending from $k \sim 2\pi E_o$ to values of $k$ just below the dissipation scales. This is consistent with the direct coupling of the pump to the collapsing cavitons. For $\omega_o$ sufficiently large the injection spectrum has a completely different character, as discussed in Sec. 7, from which we conclude that the cavitons are driven by the low lying free modes, which are driven up by the pump, and not driven directly by the pump.

Detailed studies of SLT driven by long wavelength negative damping[12] (beam instabilities) also seem to clearly demonstrate that cavitons are locally nucleated in preexisting density wells but the nucleation coupling is to the driven free modes rather than directly to the negative damping source.

It is easy to see formally[21] that, because $n(\underline{x}, t)$ is generally time dependent in SLT, the modes $\underline{e}_\nu(\underline{x}, t)$ do not behave independently. This introduces, for

example, an additional term $-i\sum_{\nu}\int d^D x \underline{e}_o^*(\underline{x},t)[d/dt\ e_\nu(x,t)]h_\nu(t)$ on the right hand side of (14) involving the time derivative of the eigenstate $e_\nu$ and therefore couples the amplitude $h_o$ to other amplitudes $h_\nu$. It was shown in I that this leads to a coupling of bound (or localized) states to free mode states. When a caviton collapses it radiates away some energy in the form of free modes. This is a relatively weak effect for $\omega_o \lesssim 0$ but accounts for the presence of both free mode and caviton contributions in the power spectrum of fluctuations (Section 6).

The tunneling of trapped modes through the density barrier, discussed above where $\lambda_\nu > 0$, is another way that free or extended modes can communicate with localized modes. The two kinds of coupling are different since the first mechanism, depending on $d/dt\ \underline{e}_\nu$, is observed[21] to occur even for $\omega_o < 0$ where there is no tunneling. As $\omega_o$ increases the tunneling mechanism probably becomes dominant.

It is interesting to observe that a free Langmuir wave incident (in the scattering sense) on a potential well plus a barrier can undergo resonance scattering when the (quantization) condition - $2\int_o^{x_\nu} dx\sqrt{\lambda - n(xt)} = (N+\frac{1}{2})\pi -$ is satisfied where now we take $\lambda = k^2$ to be the energy of the incident free mode. When this condition is satisfied the wavefunction inside the well is much larger than that outside (and there is perfect transmission of the incident wave in one dimension). In the Langmuir wave problem the PMF of the resonance-enhanced confined wavefunction in the well could nucleate collapse. It will be interesting to see if this resonance scattering phenomena can account for the nucleation of caviton fields by low lying free modes in time dependent density wells.

## 7. Power spectra of turbulent fluctuations for $\omega_o < k^2$

The power spectra $|E(\underline{k},\omega)|^2$ and $|n(\underline{k},\omega)|^2$ of the turbulent fluctuation time series are a very useful diagnostic of SLT dynamics. In Fig. (5) are shown $|E(\underline{k},\omega|^2$ for various values of k where the direction of $\underline{k}$ is at an angle of 45° from the x axis which is the direction of $\underline{F}_o$. The spectra consist of two main features: a broad continuum supported by frequencies generally less than $\omega = 0$ (frequencies are measured from the heater frequency $\omega_o$=5 in these Figures), and a sharper but weaker feature at positive frequencies. The broad spectrum for $\omega \lesssim \omega_o$ is the "caviton continuum;" it arises from the caviton dynamics of nucleation-collapse-burnout. The extent of this spectrum toward negative frequencies reflects the depth of collapse and the negativity of the eigenvalue $\lambda_o(t)$.[9,21] The positive frequency "free mode peak" is at exactly the free Langmuir wave frequency. [In the case of Fig. 5 a weak magnetic field along the x axis was included so that the free Langmuir frequency is $\omega = k^2 + \Omega^2\ \sin^2\theta$ where in our units $\Omega^2 = \frac{1}{2}(\omega_c^2/\omega_p)(\eta m_i/m_e)$ with $\omega_c$ the electron gyro frequency and $\theta$ is the angle between $\underline{k}$ and $B_o$.]

In 1988 Cheung and coworkers[30] investigated the turbulence induced in the ionsophere shortly, (within 30 ms), after the turn-on of a powerful HF wave which was periodically turned on and off, the off periods being much longer than the on periods. Examples of the spectra of the Langmuir fluctuations which they observed with 1 ms long pulses of the Arecibo Thomson scattering radar are shown in Fig. 6. There is remarkable qualitative and quantitative agreement between the theoretical (numerical) spectra and the observed spectra. Space does not allow us to discuss the many detailed comparisons with theory which have been made in this and subsequent experiments.[30,21]

These observations are a dramatic verification of the predictions of SLT theory since WTT cannot account for *any* aspect of these observations.

It has recently been observed[31] that when the radar observations are made with a longer delay after the turn-on of the HF pump the turbulent layer spreads out to fill an altitude layer about 1 to 2 km thick below the reflection altitude. This coincides with qualitative and quantitative changes in the Langmuir fluctuation power spectrum; an example is shown in Fig. 7.

## 8. Coexistence of parametric decay cascades and Langmuir collapse

Spectra of the type shown in Fig. 7 have long been associated with a cascade of parametric decay processes of the type discussed in Section 2. WTT was used to describe this process but it has become increasingly clear that it is, at most, only qualitatively correct and that it fails to describe several features of the observations. For several years it was believed that the *altitude* of the turbulence producing spectra like Fig. 7 was inconsistent with a decay cascade of free Langmuir waves. Very recent experiments[31] have shown that this is probably not true. To understand these experiments we have recently undertaken a study of SLT, with parametric drive at densities well below the critical or reflection at which the matching condition for parametric decay can be satisfied.

For the primary decay of the pump, which we assume to be spatially uniform, we have the matching condition

$$\tilde{\omega}_o \;=\; \omega_p(z_1)(1 \;+\; \frac{3}{2}\,(\tilde{k}\lambda_D)^2) \;+\; |\tilde{k}|c_s \qquad (16)$$

which determines $\omega_p(z_1)$ the electron plasma frequency at the "matching" altitude $z_1$, in terms of the radar-observed k.

In Fig. 8 we show time-averaged electrostatic energy spectra in the well-developed, quasi stationary turbulent state $\langle|E(k)|^2\rangle$ as a function of the magnitude of k and its angle $\theta$ with the geomagnetic field. The heater $\underline{E}_o$ and the geomagnetic field $\underline{B}_o$ are in the x direction. The simulations used a $(256\times128)$ grid in $(k_x, k_y)$ space where $\Delta k_x = \frac{2\pi}{L_x} = \frac{1}{2}\,k*, \Delta k_x = \frac{2\pi}{L_y} = \frac{\sqrt{3}}{2}\,k*$ where

$k* = \sqrt{1-\nu_i^2} = .96$, in our dimensionless units, for an ion acoustic damping parameter, $\nu_i = \frac{Im\omega_i}{Re\omega i} = 0.280$. [In physical units $k* = .96\ (2/3)\ (m_i/m_e)^{1/2} k_{De}$.] This allows us to adequately resolve the decay cascade and the small scales of collapse.

We note that in addition to the cascade peaks at $k_1 = 7.68, k_3 = k_1 - k_* = 6.72$ and $k_5 = k_1 - 2k_* = 5.76$, there is a broad background of turbulence which contains a significant fraction of the turbulent electrostatic energy and which is not accounted for in WTT. We will refer to this set of modes $k_1, k_3, k_5$, as the *primary cascade* which results from the decay of the pump. The notation 1:3:5: - - - is used because the decay conditions (5) and (6) imply that the *frequencies* of these modes will be shifted by 1,3,5 - - units of the ion acoustic frequency, $|k_1|c_s$, below the pump frequency. There is also an apparent enhancement in the zero-frequency-shift mode at $k_o = 8.16$ and in the anti-Stokes mode at $k_a = k_1 + k*$ = 8.64. In Fig. 8 we also show, for the same parameters, the time averaged ion fluctuation energy spectrum $\langle |n(k)|^2 \rangle$. Again this is dominated by a broad spectrum associated with collapse but also contains a sharp feature at $k_1 = 7.68$ associated with the primary decay of the pump.

In Fig. 9 we show the power spectra $|E(\underline{k},\omega)|^2$ for $k_y = 0$ (corresponding to $\theta = 0$) and for several values of $k_x$ including two of the three primary decay-resonant values $k_1 = 7.68, k_3 = 6.72$. [Note that the cascade proceeds along $k_x$ in the steps $k_1 \rightarrow -k_3 \rightarrow +k_5$ etc. but, since - k, is equally likely to be excited in the primary decay, the spectra are *on the average* symmetric between $\underline{k}$ and - $\underline{k}$.] The power spectra consist of free mode peaks at $\omega \simeq k_x^2$, (In physical units at $\tilde{\omega} - \omega_p \simeq 3/2(k_x\lambda_D)^2\omega_p$), imbedded in a weaker broad continuum. This continuum is more prominent in the modes not in the primary cascade such as $k_x$ = 3.36, 7.20 and 8.64. The free mode peaks at the primary cascade values, $k_x = k_1, k_3, k_5$, are enhanced over the peaks for neighboring k values consistent with the enhancement of these modes in the energy spectrum of Fig. 7. The broad background in the power spectra is due to caviton excitations. This background is relatively weak compared to the free mode peak for $k^2 < \omega_o$ and relatively much stronger for $k^2 > \omega_o$.

In Fig. 9 we also show ion fluctuation (ion line) power spectra, $\langle |n(\underline{k},\omega)|^2 \rangle$, for the same parameters. Note that these consist of (usually) unequal wings at $\omega = \pm kc_s$ associated with free ion acoustic waves and a central feature near $\omega = 0$, as in the observed spectra.

In Fig. 10 we show the maximum electric field $|\underline{E}(\underline{x},t)|^2_{max}$ in the simulation cell as a function of time. The sharp peaks are associated with caviton events. In Fig. 10e,f,g we show the time series of the modulus square Fourier coefficients of the density fluctuations, $|n(k,t)|^2$. Note that there is a positive correlation of the peaks in $|n(k,t)|^2$ with the caviton event in Fig. 10d which is consistent with our claim that collapse is the primary source of ion fluctuations. For even higher values of k (not shown) the correlation is nearly 100%. Other diagnostics show that most of the electrostatic energy is dissipated by caviton collapse.

We can get a better estimate of the fraction of energy involved in caviton collapse compared with the energy in free modes by looking at the time histories

of $|E(k,t)|^2$ for various Fourier modes. Some examples are also shown in Fig. 10a,b and c. Notice the fast modulations or "buzzes" on these signals, which occur during the collapse periods, as can be verified by comparison with Fig. 10d.

We can interpret these signals by writing the total electrostatic envelope field $\underline{E}(\underline{x},t) = \underline{E}_c(\underline{x}t) + \underline{E}_f(\underline{x}t)$ where $\underline{E}_f(\underline{x},t)$ is the nonlocalized or free mode part. The same two component ansatz for $\underline{E}$ was made in I (and in refs. 7 and 8) where $\omega_o \lesssim 0$ and a similar approach has recently been used to describe beam driven SLT.[12] Here we can get a microscopic description of this decomposition from the power spectra and from the following argument: The localized or caviton part, $E_c$, can be written as a sum over $N(T)$ discrete events occuring during the observation time T [see I.]

$$\underline{E}_c(x,t) \;=\; \sum_{i=1}^{N(T)} \underline{\varepsilon}_i(x - x_i, t - t_i) \tag{17}$$

With this decomposition we can write for the Fourier modes

$$\begin{aligned} |E(\underline{k},t)|^2 \;&=\; |E_f(\underline{k},t)|^2 + |\underline{E}_c(\underline{k},t)|^2 \\ &+ \sum_i 2|\varepsilon_i(\underline{k},t)||E_f(\underline{k},t-t_i)|\,\cos(\omega_k t - \underline{k}\cdot\underline{x}_i - \phi_i(t)) \end{aligned} \tag{18}$$

where we have written $E_f(\underline{k},t) = |E_f(\underline{k},t)|\,\exp\,-i\omega_k t$, where, from the observed power spectra, $\omega_k$ is close to the Bohm-Gross frequency. The caviton phase [I] $\phi_i(t)$, obtained from $\varepsilon_i(kt) = |\varepsilon_i(k,t)|\,\exp\,i\phi_i(t)$, is a rapidly varying 'chirpped' phase arising from the nucleation and collapse of cavitons.[21] The 'buzzes' in the $|\underline{E}(\underline{k},t)|^2$ can be identified with the rapidly varying interference terms in (18). From this and from estimates of the fraction of power in the broad caviton background in the power spectra we can estimate the fraction of the time averaged electrostatic energy in free modes compared to that involved in collapse. We find, roughly, that in the case of the parameters of Fig. 8-10 that at low k ($k^2 \ll \omega_o$) about half of the total time averaged energy is in free modes while for $k^2 > \omega_o$ the fraction of free mode energy decreases from about 50% to zero as k increases. A more complete discussion of this point will be published elsewhere. For smaller, including negative, values of $\omega_o$ the relative fraction of energy in collapsing, localized states increases dramatically.

Thus we have evidence that at underdense altitudes a decay cascade can coexist with caviton collapse. Under these conditions the primary energy dissipation is through caviton collapse but a large fraction of the time average electrostatic energy is contained in free modes.

The value of $E_o = 0.6$ used in the examples here is about half the value typically used in I for the near critical density studies. This corresponds to physical

$\tilde{E}_o \lesssim .3V/m$ which is well above decay instability thresholds. If $E_o$ is increased to $E_o = 1.2$ the level of caviton activity is much greater, the distinct cascade structure disappears and the nonresonant neighbor modes of the primary 1:3:5 modes are nearly equally excited. We believe this can be understood in terms of the increased damping of free modes due to their interaction with cavitons and with their induced scattering from the density fluctuations resulting from burnout cavitons. The damping of free modes due to the nucleation of cavitons is discussed below.

The level of ion density (ion acoustic) fluctuations observed in the simulations is much larger than assumed by conventional WTT treatments. WTT estimates that the enhanced level of ion fluctuations will be small, because of the Manley-Rowe relations obeyed by the parametric instability, and locally distributed in narrow regions of k space, e.g. at $k \sim k_1, 2k_1 - k*, 2k_1 - 3k*$, etc. These peaks are observed in $\langle |n(k|^2 \rangle$ (Fig. 8) but do not account for a major part of the ion fluctuation energy. We attribute the spectrum and level of ion fluctuations to density cavities remaining from collapse. This is consistent with the level of collapse deduced from other properties.

The high level of ion density fluctuations implies that the sound wave induced scattering of Languir waves from ion fluctuations is important here. From studies of renormalized turbulence theories[32] we can abstract a renormalized, steady state balance equation for free Langmuir waves (FLW's) of the form

$$\gamma_L(\underline{k}) W_f(\underline{k}) \;=\; S_L\{W_f, \underline{k}\} \tag{19}$$

where $W_f(\underline{k})\delta(\underline{k} - \underline{k}') = \langle \underline{E}_f(\underline{k}, t)\underline{E}^*_f(\underline{k}', t)\rangle$. The total free mode (linear plus nonlinear) damping can be written

$$\begin{aligned}\gamma_L(\underline{k}) \;&=\; \nu_e(\underline{k}) + (\pi/2)|\hat{\underline{k}} \cdot \underline{E}_o|^2 R_n(\underline{k}, o) + (\pi/2) \int d\underline{k}'(\hat{\underline{k}} \cdot \hat{\underline{k}}')^2 W_f(\underline{k}') R_n(\underline{k}, \underline{k}')] \\ &+\; (1/4) \int d\underline{k}'(\hat{\underline{k}} \cdot \hat{\underline{k}}')^2 \langle |n(\underline{k} - \underline{k}', k^2 - k'|^2)|^2 \rangle + \nu_{cav}\end{aligned} \tag{20}$$

where $R_n = (k^2 - k'^2)\{[(k^2 - k'^2)^2 - |\underline{k} - \underline{k}'|^2]^2 + 4(k^2 - k'^2)^2 \nu_i^2(\underline{k} - \underline{k}')\}^{-1}$, and $d\underline{k}' \equiv d^D k'(2\pi)^{-D}$. The nonlinear source term is

$$S_L\{W_f, k\} = |\hat{\underline{k}} \cdot \underline{E}_o|^2 \langle |n(\underline{k}, k^2 - \omega_o)|^2 \rangle + \int d\underline{k}'(\hat{\underline{k}} \cdot \hat{\underline{k}}')^2 \langle |n(\underline{k} - \underline{k}', k^2 - k'^2)|^2 W_f(\underline{k}') + S_{cav} \tag{21}$$

In interpreting these equations it is important to note that k in these equations is expressed in units of $k*$ and to remember that in the envelope approximation and the conventional scaled units the Langmuir wave frequency is $\omega_k = k^2$ and the ion wave frequency is $\omega_s(k) = |\underline{k}|$ so that the usual decay matching conditions can be written $k^2 = k'^2 \pm |\underline{k} - \underline{k}'|$.

In these expressions no assumptions have been made concerning the form of the density fluctuation spectrum which will take to be that observed in the simulations. In particular, we do not make the usual linear dispersion assumption of WTT that $\langle|n(\underline{k},\omega)|^2\rangle = n_s(\underline{k})2\pi\delta(\omega - |\underline{k}|) + n_s(-\underline{k})2\pi\delta(\omega + |\underline{k}|)$.

The first term in (20) is the linear (collisional plus Landau) damping, the second term the parametric gain (Stokes) or loss (antiStokes) induced by the pump, the third term contains the gain and loss from Langmuir-induced scattering from equilibrium ion density fluctuations, and the last term, which is neglected in conventional treatments, is the scattering-out rate due to ion fluctuation induced scattering of FLW's from enhanced ion fluctuations. [Except for the explicit pump terms, all of these contributions in the linear dispersion, WTT limit for D=1 are given in Payne et al.[33]]

In the conventional WTT treatment of the cascade, the source terms are neglected altogether and a singular spectrum results from the balancing of the linear damping against the second and third terms in (20). This leads to the well-known cascade solutions.[34] The number of steps in the cascade is roughly $m = |E_o|^2/|E_{ot}|^2$ where $|E_{ot}|^2 \simeq \nu_e(k_1)\nu_i$ is the threshold field for the PDI.[16] In our simulations $m \gg (k_1/k_*)$ so conventional WTT would predict an unlimited cascade to k=0. The ion sound wave induced scattering of FLW's from enhanced ion fluctuations, the final term in (20), has the effect of replacing $\nu_e$ by $\nu_{eff}$, which is the sum of $\nu_e$ and this final term; since $\nu_{eff} > \nu_e$ this induced scattering from enhanced ion fluctuations reduces the number of steps in the cascade.

The source terms also play an important role. In (21) the first term is the source at the Langmuir frequency, $k^2$, due to the beating of the pump with the turbulent ion fluctuations and the last term the ion fluctuation-induced scattering-in term. The ion density (ion line) power spectra in $\langle|n(\underline{k},\omega)|^2\rangle$ in Fig. 9 have, in addition to the familar peaks at $\omega = \pm kc_s$, a broad feature at $\omega = 0$. We identify this with the ion density fluctuation during collapse which is driven by a ponderomotive force (PMF) which has a power spectrum centered at $\omega = 0$ and a width $\Delta\omega \lesssim 2\pi/\tau_c$ where $\tau_c$ is the caviton lifetime. Such an enhanced $\omega = 0$ feature has been observed at Arecibo[36,37] and is not accounted for in WTT. The peaks at $\omega = \pm kc_s$ are generated by the free ion sound waves radiated following collapse or by the decay interaction.

The spectral features of the ion line are essentially independent of $\omega_o$, i.e. of altitude, unlike the features of the plasma line. The three peaks in the ion line power spectrum produce three peaks in the pump beat-source term in (21), at $\omega_k = \omega_o \pm kc_s$- corresponding to the Stokes ($k = k_1$) and antiStokes ($k = k_a$) line and for $|\omega_k - \omega_o| < \Delta\omega$ corresponding to the "OTSI line." Note that the $k_x$ values associated with each of these resonances is excited above the background in $\langle|\underline{E}(\underline{k})|^2\rangle$, Fig. 8. The Stokes or decay line mode, $k_1$, is most strongly excited because its damping is reduced by the parametric decay coupling to the pump in (20) whereas the damping for the anti-Stokes line is *increased*. The OTSI mode *damping* is, to first approximation, uneffected by direct coupling to the pump. The modes excited by this beat source term at $\omega_k \simeq \omega_o$ initiate secondary cascades to lower k. Signatures of this source term are particularly clear in the

power spectra of modes *not* in the primary cascade such as $k_x = 0.36$ in Fig. 9. The cascades originating near $k_o$ are independent of the primary decay cascade originating from $k_1$ and appear to produce the free-mode component of the modes in the energy spectrum $\langle|\underline{E}(\underline{k})|^2\rangle$, which lie between the primary cascade modes.

At lower k values, the cascades die out and the ion fluctuation induced-scattering terms become dominant. Part of the low k spectrum is also due to localized caviton excitations.

The primary free Langmuir wave (LW) cascade is initiated by the pump (heater) and Langmuir energy tends to flow toward low k. The parametric decay process driven by the pump produces LW's at $\pm\underline{k}_1$ and $\pm\underline{k}_3$ and $\pm\underline{k}_5$, etc. In the early time development of the PDI from quiet initial conditions these modes form *standing* LW's which have a ponderomotive force with spatial periods $\pi/k_1, \pi/k_3$, etc. This PMF digs a train of density cavities with the same period.

The long wavelength LW's resulting from these cascades can drive the nucleation of trapped Langmuir fields in preexisting cavities which then proceed to collapse and burnout. The preexisting cavities may be generated from the standing LW's, as mentioned above, or from previous burntout collapses. The collapsing cavitons emit hot electrons, a broad spectra (in k) of ion waves and a broad spectrum of free modes. These ion waves and free modes interact in the decay and induced scattering processes. Again, these cascades in general do not coincide with the primary cascade ($k_1, k_3, k_5 - - -$) driven directly by the pump.

The long wavelength LW's resulting from the cascades are expected to be much more efficient in driving the nucleation of new trapped electric fields in preexisting density cavities, in these underdense regimes, than is the pump field, whose frequency is too high relative to the local cavity resonance frequencies.

Various diagnostics, including the calculated injection spectrum[6], indicate that direct nucleation by the pump is not important in this regime. In I we stressed the analogy of Zakharov's equation for $\underline{E}$ with Schrödinger's equation were the density fluctuation, n($\underline{x}$,t), plays the role of a potential. The density debris from burntout cavitons will generally consist of localized density cavities surrounded by enhanced density shoulders producing a barrier-plus-well potential. We make the conjecture that the nucleation of new electric fields in the burntout wells is through a resonant scattering of free modes from such potentials; a process well-known in quantum mechanics.[38] The free mode frequencies, $\omega_k = k^2$, for low values of k can resonate with rather shallow potential wells, in which case the Langmuir wave function inside the well becomes very large and can produce a strong PMF leading to another collapse. This free mode-caviton coupling is formally accounted for by the terms $\nu_{cav}$ and $S_{cav}$ in (20) and (21). At this point we do not have explicit expressions for them. Since most of the energy is dissipated by caviton burnout, it follows from simple energy balance estimates that $\nu_{cav} \sim \langle D\rangle/\langle W_f\rangle$ where $\langle D\rangle$ is the observed dissipation rate, $\langle D\rangle \simeq \sum_{\underline{k}} \nu_e(k)\langle|\underline{E}_c(\underline{k}|^2\rangle$, and $\langle W_f\rangle$ is the average energy density in free modes, $\langle W_f\rangle = \sum_{\underline{k}}\langle|\underline{E}_f(\underline{k})|^2\rangle$; both of these quantities may be estimated from the simulations. For weaker driving ($E_0$=0.6) the widths of the lowest k free mode peaks in $\langle|\underline{E}(\underline{k},\omega)|^2\rangle$ appear to be at least a factor of 2 greater than for the primary

cascade modes and the widths imply $\gamma_L(\underline{k}) \gg \nu_e(\underline{k})$ for all k's $\lesssim 10$. For stronger driving ($E_o \sim 1.2$) (spectra not shown here) the lines are dramatically broadened to the extent that free mode peaks are not clearly identifiable. This broadening is consistent with the scenario outlined above but the relative contributions of $\nu_{eff}(k)$ and $\nu_{cav}$ still need to be determined. Further detailed parameter studies are needed to validate this theoretical description of the numerical data. This smoothing of the spectrum is also consistent with the transition from discrete to continuous spectra, with increasing laser intensity, in the second harmonic emission spectra arising from the PDI, in laser-plasma interactions, as discussed by H. Baldis and P. Young in their contribution to these proceedings.

The radars, of course, measure only fixed values of $\underline{k}$. The observed frequency cascade power spectra must arise as an altitude integrated effect. A complete altitude integrated spectrum requires a model for the altitude dependence of the electron density, of the heater profile and a series of simulations for a range of $\tilde{\omega}_o$ values. At most altitudes the primary cascade peaks cannot contribute to the integration for the fixed value of $\underline{k}$ but the background turbulence can. In the integration this background provides the observed enhanced background on which the sharper cascade structures sit. For stronger driving the 3: and 5: cascade peaks become less distinct and the background becomes stronger. We believe that the combination of these effects in the integrated spectrum may account for the often observed "broad bump" in the Arecibo spectra.[37] Note that at every altitude there is a beat source for Langmuir excitations at frequency $\omega$ which is just the first term in (21) where the frequency argument is $\omega - \omega_o$ (rather than $k^2 - \omega_o$). The three peaks in $\langle |n(\underline{k},\omega - \omega_o)|^2 \rangle$ produce sources at $\omega = \omega_o$ and $\omega = \omega_o \pm |k|c_s$. Only at special altitudes, for fixed $\underline{k}$, will these sources coincide with the free mode resonances at $\omega = k^2$. Because of this nonresonant excitation, the altitude integration will *enhance* the decay line, the zero frequency shift (OTSI) line and the antiStokes line!

## 9. Caviton correlations and a caviton gas model

In Section 5 we mentioned that in the case of overdense driving, $\tilde{\omega}_o = \tilde{\Omega}_o - \omega_p < 0$, for relatively strong ion wave damping, individual cavitons can become locked in limit cycles of nucleation, collapse and burnout. In I we presented preliminary evidence, from D=2 Zakharov simulations, that in such regimes the caviton gas could undergo transitions to states of high temporal and spatial order. This order produces distinctive line structure in the spectra $|E(\underline{k},\omega)|^2$ and $|n(\underline{k},\omega)|^2$ which was discussed in I and will not be repeated here.

Here we outline the elements of a caviton gas model which elucidates the mechanisms of caviton interactions leading to correlations. This model reproduces several features of the full simulations and allows us to treat systems with many more cavitons.

We assume, for purposes of this discussion, that $\lambda_o(max) < \omega_o < 0$, and the collapsing caviton gas is weakly coupled. For simplicity, we also restrict detailed discussion to a scalar version of Zakharov's equations.[21].

The energy density of free modes, $W_f = < |E_f|^2 >$, decreases rapidly as one considers plasmas which are increasingly overdense. This is because the caviton-free mode coupling becomes increasingly non-resonant. However, the production of ion acoustic waves is relatively insensitive to the plasma density. Therefore, in this regime, the coupling is primarily due to acoustic waves.

Since the cavitons are weakly coupled, we seek a perturbation theory in which the zeroth order state is one of uncoupled collapsing cavitons, each of which is executing the same stable limit cycle. This state is described by the spatial position, $x_i$, and collapse time, $t_i$, of each caviton, where, e.g., $|E|^2$ of the ith collapse varies as $F(x - x_i, t - t_i) = F(x - x_i, t - t_i + \tau)$ where $\tau$ is the cycle time. Let $t_i = n\tau + (\theta_i/2\pi)\tau$ with $0 < \theta_i < 2\pi$. Then we may describe the ith cycle by $x_i$ and $\theta_i$, the "collapse phase." The dynamics of the caviton gas will consist of the equations of motion for its state variables. (Note: for the real vector model of Langmuir waves, each collapse also has a direction which is needed for a complete specification of the state.)

The assumption that the caviton coupling is weak is taken to mean that the state changes slightly in a time $\tau$. Therefore, the acoustic waves impinging on a given caviton, which consists of the superposition of the emission of sound waves from previous collapses of all other cavitons, may be taken to be periodic in time over the time scale of a few collapses.

Ion acoustic damping and geometrical attenuation imply that the coupling between all but nearby neighbors is negligible.

We also assume that the cavitons are separated by at least a few caviton diameters so that the acoustic perturbation from any single caviton may be approximated by a plane wave over the width of the given caviton. Its wavelength, $\lambda$, is simply the product of the ion acoustic speed (renormalized by the ion acoustic damping), $c_s$, and $\tau$.

A natural perturbation theory seeks to superpose the effect of all such plane acoustic waves. The response $(\delta x, \delta\theta)$ of the caviton in state $(x, \theta)$ to a given small amplitude wave, $\delta n$, is linear in the amplitude of the wave. The only parameter it can depend on is the relative phase, $\phi - \theta$ where

$$\delta n(y,t) \sim \cos(k(y-x) - \omega t + \phi)$$

and $k = 2\pi/\lambda$ , $\omega = 2\pi/\tau$. Because of the nearly singular nature of the collapse cycle, the determination of this response function is nontrivial. It has been numerically determined for a one dimensional version of the Zakharov equations which allow for collapse. The results are remarkably close to what is obtained from the following heuristic argument:

Since the acoustic dynamics is linear in the density, the only direct effect an external acoustic wave has on a collapse cycle is through its effect on the Langmuir waves which are trapped in the caviton. This effect is most important when the relative size of $\delta n$ is largest compared to the unperturbed caviton depth. The evolution of the Langmuir wave phase, which is crucial in determining the coupling to the heater field, can be taken to depend on $\lambda_o(t) + \delta n(x,t)$. Let $\lambda_o$

attain its smallest value at a time $\tau\psi/2\pi$ into the collapse cycle. We expect the response of $\theta$ to depend primarily on the value of $\delta n$ at that time. Therefore one might guess that

$$\delta\theta \sim \cos(\phi - \psi - \theta) \tag{22}$$

The response of the caviton location can only depend on the gradient of $\delta n$. Again, it is the gradient at a time $\tau\psi/2\pi$ into the collapse cycle which is most important. Therefore we expect that

$$\delta x \sim k \cos(\phi - (\psi + \mu) - \theta) \tag{23}$$

where $\mu \sim \pi/2$, because the gradient of $\delta n$ peaks at a phase which differs by $\pi/2$ from the phase at which $\delta n$ peaks. As mentioned above, the numerically determined linear response is very close to this heuristic result. The numerically determined coefficients in these relations have the property that the response of the collapse phase, in units of $2\pi$, is orders of magnitude larger than the response of the collapse location, in units of a caviton diameter. This may be interpreted as being due to the combined inertia of Langmuir waves and ion fluctuation which make up the caviton, which resists acceleration by the gradient of $\delta n$, while the caviton phase primarily depends only on $\lambda_o(t)$. (Note: Because of Langmuir wave burnout and acoustic wave emission, the caviton momentum is effectively lost at the end of the caviton cycle, allowing a complete description in terms of $(x, \theta)$.

The one remaining step in the derivation of the caviton gas model is the determination of the acoustic waves a distance r away from a periodically collapsing caviton. Asymptotically large r is not appropriate because the wave amplitude is a rapidly decreasing function of r and it is only within a few caviton radii that its amplitude is large enough to matter. If one assumes that during that portion of the caviton cycle, during which most acoustic emission occurs, the caviton size is small compared to r, then one may model the emission process as being caused by a point ponderomotive force. If one also assumes that the emission effectively takes place during a time interval short compared to $\tau$, then one has the "impulse model" for acoustic production. In this case, it has been numerically determined, that the following is a good fit to the acoustic emission from a caviton with collapse phase $\theta$ in three dimensions:

$$\delta n(rt) = \frac{IA}{(r/\tau c_s)^\alpha} \cos[kr - \omega t + \theta] \tag{24}$$

where A $\sim$ 100, $\alpha \approx 8$, and the impulse $I = \int_t^{t+\tau} dt N(t) dt$ and $N(t)$ is the caviton Langmuir wave energy. If one relaxes the ansatz about the short emission duration, then $\theta$ is replaced by $\theta$ plus a constant, and I is somewhat reduced in amplitude. Since this is the same for all cavitons, it can be suppressed by redefining $\theta$ and the scale of time for evolution of the caviton gas. The above fit is good for $2 < r/\tau c_s < 4$. Because $\delta n(rt)$ decreases rapidly for $r/\tau c_s > 4$,

and because $\alpha$ is large, there is no harm in using the above fit for larger r. For $r/\tau c_s$ <2, $\delta n$ rapidly becomes so large that the linear response model breaks down. It has been observed in two dimensional simulations of Zakharov's model that two cavitons will merge in about a single caviton cycle time if they approach each other to within a few caviton radii. We use this empirical observation to supplement the caviton dynamics by a merging rule which replaces a caviton pair by a single caviton half way between the two, with a random collapse phase, if the pair spacing is less than some cutoff value and their relative displacement would move them closer in the next collapse cycle. The imposition of a random phase must be regarded as adhoc. There are regimes, however, where merging events are rare, so at least in those regimes, this adhoc feature may not be fatal.

Finally, equations (22), (23), and (24) imply, in the weakly coupled regime where caviton-caviton interactions may be superposed, that the caviton state after n+1 collapses $(\underline{x}_l^{n+1}, \theta_l^{n+1})$; is related to the state after n collapses by

$$\underline{x}_l^{n+1} = \underline{x}_l^n + B\sum_{j\neq l} \frac{\underline{r}_{lj}^n}{r_{lj}^n} \cos[kr_{lj}^n + \theta_j^n - \theta_l^n - (\psi+\mu)]/(r_{lj}^n)^\alpha \qquad (25)$$

where $\underline{r}_{lj}^n = \underline{x}_l^n - \underline{x}_j^n$, and $r_{lj}^n = |\underline{r}_{lj}^n|$

$$\theta_l^{n+1} = \theta_l^n + C\sum_{j\neq l} \cos[kr_{lj}^n + \theta_j^n - \theta_l^n - \psi]/(r_{lj}^n)^\alpha \qquad (26)$$

where $C \sim IA(\tau c_s)^\alpha$ and $B \approx C/100$. The proportionality coefficients depend on properties of the individual caviton cycle. For this model to be consistent with the superposition ansatz, the initial conditions must be such that, for definite values of B and C, the change in the caviton state must be small in any one collapse cycle.

This model has a very rich structure. It turns out that, apart from initial conditions, $\mu$ is the only parameter which affects the qualitative properties of the evolution. While $\mu \approx \pi/2$, very different behavior is obtained depending on whether $\mu > \pi/2$, or $\mu < \pi/2$. A consideration of the two caviton model suffices to illustrate this point.

Let $y = |x_1 - x_2|$ and $\zeta = \theta_1 - \theta_2$. It can be shown that for $\pi/2 < \mu < 3\pi/2$, there are two stable fixed points: $ky = \psi + \mu + \pi/2, \zeta = 0$; and $ky = \psi + \mu + 3\pi/2, \zeta = \pi$. It is understood that changing $ky$ by $2\pi$ yields another fixed point with the same stability properties. Which of this pair of stable fixed points is obtained depends on initial conditions. The one at $\zeta = O$ has both cavitons collapsing in unison, while the one at $\zeta = \pi$, has alternating collapses. For $-\pi/2 < \mu < \pi/2$ there are no stable fixed points, but there are separatrices which bound the motion in y. However, if there are perturbations to the motion, for example a third caviton, these separatrices would be crossed and there would be no simple constraint on how large or small y could become.

Figure 11 illustrates the generation of collapse phase correlations between different cavitons in a multicaviton case. The initial state had no such correlations, but the cavitons were initially placed on a nearly regular square lattice. These correlations were strong after 10 collapses. Because the caviton motion is slow compared to its phase dynamics, 1000 collapses were followed to show that some degree of spatial regularity is retained after a time long enough such that spatial motion is significant. Note that the phase correlations are still strong even though the spatial distribution of cavitons is somewhat irregular.

## 9. Concluding remarks

The set of concepts outlined in this article has been quite successful in describing, at least qualitatively, the numerical simulations *and* several well-diagnosed experiments involving strong Langmuir turbulence. Certain of these concepts can be described in more analytical detail that we have given here. Generally, however, the analytic tools available in this subject have been quite limited. In our work we have gained understanding by considering simplified, reduced models, which themselves usually require numerical solution. It is a great challenge to theoreticians to put some more analytical "meat" on these conceptual structures.

## REFERENCES


1. V. E. Zakharov, "Collapse of Langmuir waves," Sov. Phys. JETP, 35, 908, 1972.
2. A. Y. Wong and P. V. Cheung, "Three dimensional self-collapse of Langmuir waves," Phys. Rev. Lett. **52**, 1222, 1984.
3. A. J. D. D'yachenko, A. N. Pushkarev, A. M. Rubenchik, R. Z. Sagdeev, V. F. Shvets and V. E. Zakharov, "Computer Simulation of Langmuir Collapse," Physica D (1989).
4. L. M. Degtyarev, V. E. Zakharov, R. Z. Sagdeev, G. I. Solov'ev, V. D. Shapiro, and V. I. Chevchenko, "Langmuir collapse unde pumping and wave energy dissipation," Zh. Eksp Theor. Fiz. 24, 1212-1213, 1983 [Sov. Phys. JETP58, p. 710, 1984].
5. H. A. Rose and M. I. Weinstein, "On the bound states of the nonlinear Schrödinger equation with a linear potential," Physica D, 30, 207-218, 198
6. G. D. Doolen, D. F. DuBois and H. A. Rose, "Nucleation of cavitons in strong Langmuir turbulence," Phys. Rev. Lett. **54**, 804-807, 1985.
7. D. Russell, D. F. DuBois and H. A. Rose, "Collapsing caviton turbulence in one dimension," Phys. Rev. Lett. **56**, 3-14, 1987.
8. D. Russell, D. F. DuBois and H. A. Rose, "Nucleation in Two-Dimensional Langmuir Turbulence," Phys. Rev. Lett. **60**, 581-584, 1988.

9. D. F. DuBois, Harvey A. Rose and David Russell, "Power spectra of fluctuations in strong Langmuir turbulence," Phys. Rev. Lett. **61**, 2209, 1988.

10. P. A. Robinson, D. L. Newman and M. V. Goldman, "Three dimensional strong Langmuir turbulence and wave collapse," Phys. Rev. Lett. **61**, 702, 1988.

11. P. A. Robinson and D. L. Newman, Phys. Fluids B, 1, 2319 (1989).

12. P. A. Robinson and D. L. Newman, "Two component model of strong Langmuir turbulence: Scalings, spectra and statistics of Langmuir waves,"and "Density fluctuations in strong Langmuir turbulence: Scalings, spectra and statistics," (preprints 1990).

13. C. J. Walsh, D. M. Villeneuve and H. A. Baldis, Electron plasma-wave production by stimulated Raman scattering: Competition with stimulated Brillouin scattering, Phys. Rev. Lett. **53**, 1445 (1984).

14. D. M. Villeneuve, H. A. Baldis and J. E. Bernard, Suppression of stimulated Raman scattering by seeding of stimulated Brillouin scattering in a laser-produced plasma, Phys. Rev. Lett. **59**, 2547 (1987).

15. H. A. Rose, D. F. DuBois and B. Bezzerides, "Nonlinear Coupling of Stimulated Raman and Brillouin Scattering in Laser-Plasma Interactions," Phys. Rev. Lett. **58**, 2547-2550, 1987.

16. D. F. DuBois and M. V. Goldman, "Radiation induced instability of electron plasma oscillations," Phys. Rev. Lett. **14**, 544, 1965.

17. V. P. Silin, "Parametric resonance in a plasma," Sov. Phys. JETP, Engl. Transl. 21, 1127, 1965.

18. M. V. Goldman, Ann. Phys. (N.Y) **38**, 95, (1966).

19. M. V. Goldman and D. F. DuBois, "Stimulated scattering of light from plasmas," Phys. Fluids **8**, 1404 (1965).

20. A. A. Vedenov and L. I. Rudakov, "Interaction of waves in continuous media," Sov. Phys. Dokl. **9**, 1073 (1965).

21. D. F. DuBois, Harvey A. Rose and David Russell, "Excitation of Strong Langmuir Turbulence Near Critical Density; Application to HF Heating of the Ionosphere," Los Alamos National Laboratory report LA-UR-89-1419, to be published in Journal of Geophysical Research (1990). Refered to in text as I. See also Physica Scripta **T30**, 137 (1990).

22. M. V. Goldman, "Progress and problems in the theory of Type III solar radio emission," Solar Physics **81**, 173, 1982.

23. M. V. Goldman, "Strong turbulence of plasma waves," Rev. Mod. Phys. **66**, 709 (1984).

24. D. Levron, G. Benford and D. Tzach, Phys. Rev. Lett. **58**, 1336 (1987).

25. P. A. Robinson and D. L. Newman, "Strong plasma turbulence in the earth's electron foreshock," preprint (1990).

26. G. L. Payne, D. R. Nicholson and M. M. Shen, "Numerical test of weak turbulence theory."

27. H. A. Baldis, P. E. Young, R. P. Drake, W. K. Kruer, Kent Estabrook, E. A. Williams and T. W. Johnston, "Competition between the stimulated Raman and Brillouin scattering instabilities in 0.35 $\mu$m irradiated CM foil targets, Phys. Rev. Lett. **62**, 2829 (1989).

28. S. H. Schochet and M. I. Weinstein, Commun. Math. Phys. **106**, 569 (1986).

29. H. A. Rose and M. I. Weinstein, "On the bound states of the nonlinear Schrödinger equation with a linear potential," Physica D, 30, 207-218, 1988.

30. P. Y. Cheung, A. Y. Wong, T. Tanikawa, J. Santoru, D. F. DuBois, Harvey A. Rose and David Russell, "Short time scale evidence for strong Langmuir turbulence in H-F heating of the ionosphere," Phys. Rev. Lett. **62**, 2676, 1989.

31. F. T. Djuth, M. P. Sulzer and J. H. Elder, submitted to Geophysical Research Letters (1990) (preprint) and private communication.

32. D. F. DuBois and H. A. Rose, Phys. Rev. A **24**, 1476 (1981).

33. G. L. Payne, D. R. Nicholson and M. M. Shen, Phys. Fluids **B1**, 1797, 1989.

34. D. F. DuBois and M. V. Goldman, Phys. Rev. Lett. **28**, 218, 1972a. E. J. Valeo, C. Oberman and F. W. Perkins, Phys. Rev. Lett. **30**, 1035, 1972. W. L. Kruer and E. J. Valeo, Phys. Fluids, 16, 675, 1973. J. A. Fejer and Y. Kuo, Phys. Fluids **16**, 1490-1496, 1973. F. W. Perkins, C. Oberman and E. J. Valeo, J. Geophys. Res. 79, 1478-1496, 1974. J. A. Fejer and Y. Kuo, AGARD Conf. Proc., 138, 11-1-11-8, 1974.

35. M. P. Sulzer, H. M. Ierkic, J. A. Fejer and R. L. Showen, J. Geophys. Res. **89**, 6804 (1984).

36. P. Y. Cheung, private communication.

37. J. A. Fejer, C. A. Gonzales, H. M. Ierkic, M. P. Sulzer, C. A. Tepley, L. M. Duncan, F. T. Djuth, S. Gangulys and W. E. Gordon, J. Atmos. Terr. Phys. 47, p. 1165, 1985.

38. D. Bohm, "Quantum Theory," Prentice-Hall, 1953.

## WEAK COUPLING-PERTURBATION THEORY

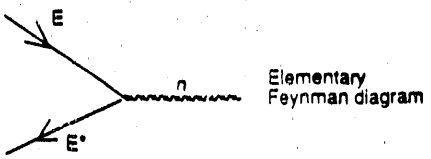


Elementary Feynman diagram

So called 'weak turbulence theory' treats the weak interaction of Langmuir waves and ion sound waves

A basic assumption: The waves satisfy the linear dispersion relations which imply the power spectra:

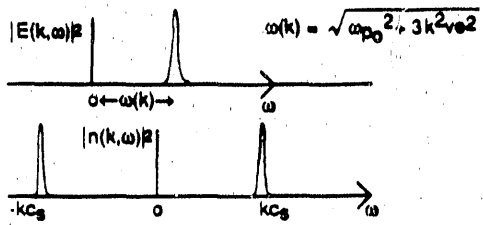


*Fig. 1.*

## MODULATIONAL INSTABILITY

- HF Langmuir waves and LF density waves are non-linearly coupled

- PMF ~ ∇|E|² Drives n (x,t)
- n (x,t) Focuses |E|²

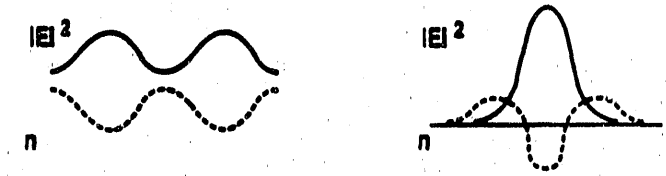


**CAVITON: HF Field Trapped in Density Cavity**

*Fig. 2.*

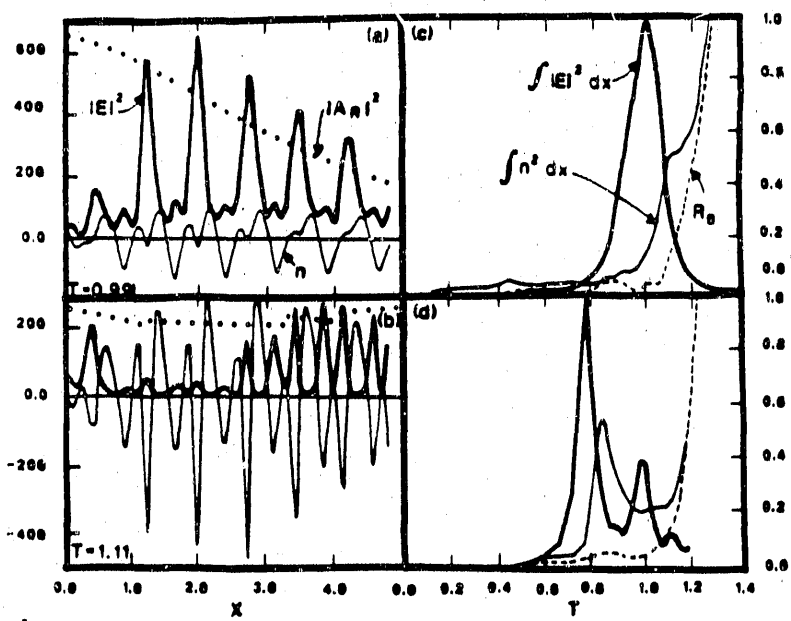


*Fig. 3.* (a),(b) Spatial profiles of $|E|^2$, $n$, and $|A_B|^2$ for various times for $n_0/n_c = 0.045$, $L = 151\lambda_0$, and $V_{osc}/c = 0.035$. The units are $4\pi n_0 T_e/459$ for $|E|^2$, $n_0/2754$ for $n$, and arbitrary units for $|A_B|^2$, $91\lambda_{0c}$ for the spatial unit, and 140 pass for the temporal unit. The total slab length was $151\lambda_0 \approx 150$ $\mu$m but we show only the leftmost portion $0 \le x \le 31\lambda_0$. (c) Temporal history of total Langmuir energy, total ion wave energy, and SBS backscatter reflection coefficient (in arbitrary units) for the case above. The unit of time is 150 ps. (d) Same but for $V_{osc}/c = 0.07$, $n_0/n_c = 0.055$. Here the unit of time is 132 ps. The mean square thermal fluctuations were $(|E|^2)_{thermal} \approx 0.1$ and $(n^2)_{thermal} \approx 900$.

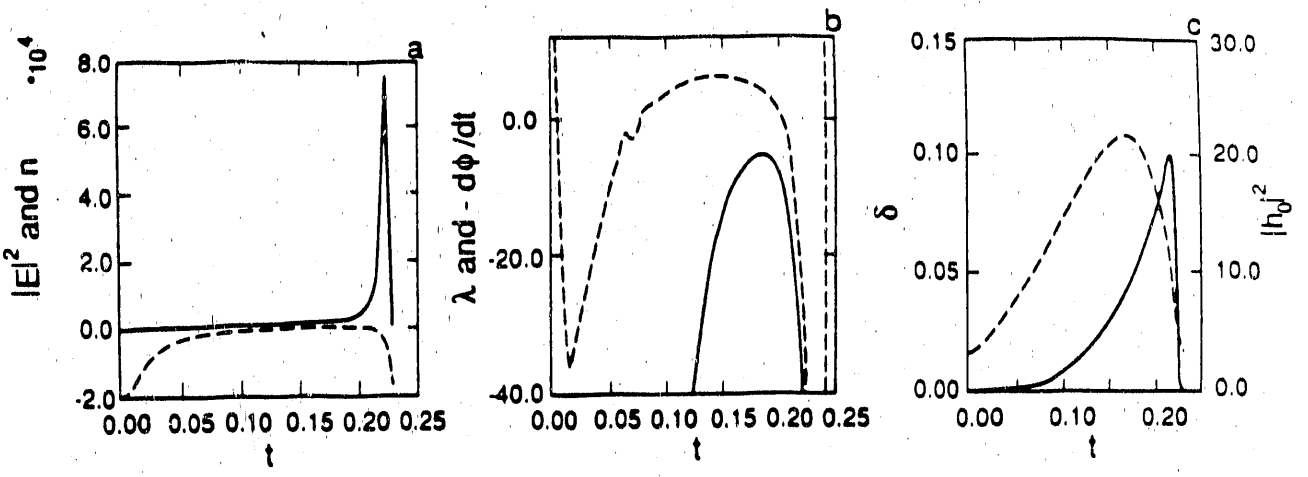


*Fig.* 4. The temporal evolution of (a) $|E(r = 0, t)|^2$ and $n(r = 0, t)$ (dashed), (b) $\lambda_0(t)$ and the phase velocity $-d\Phi/dt$ (dashed) and (c) the caviton width $\delta(t)$ (dashed) and the electrostatic energy in the cavitон $|h_0(t)|^2$ in the scalar model: $E_0 = 1.8$, $nt_i/\eta nt_e = 2 \times 10^4$, $v_i = 0.9$ and $\omega_0 = 0$.

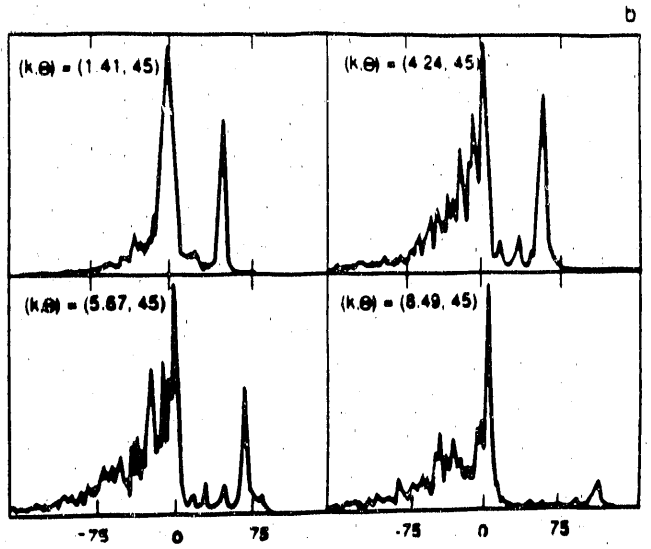


*Fig.* 5. Power spectra $|E(k, \omega)|^2 E_0 = 1.2$, $\omega_0 = 5$, $\omega_c/\omega_p = 0.2$, $L_r = L_t = 2\pi$, M = 1836. Spectra are smoothed over an angular frequency interval $\Delta\omega \simeq \pi$. Spectra intensity scales are arbitrary. The spectra are for various values of $(k, \theta)$. Because of a numerical coincidence, when these results are scaled to the more realistic value M = 9 × 1836, the frequency scales can also be read as kHz of frequency (not angular frequency).

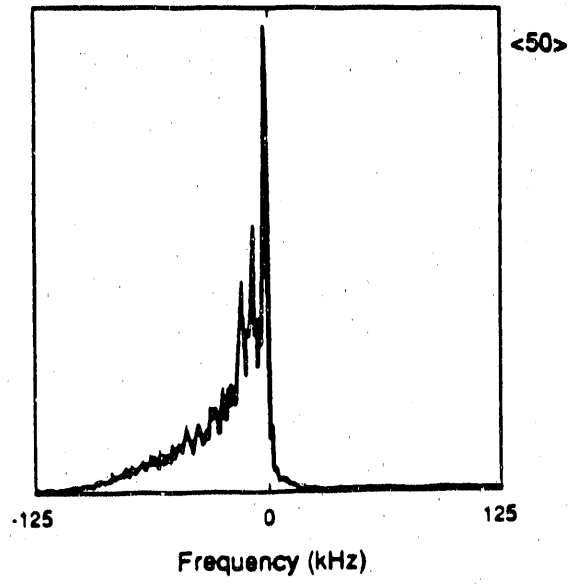


*Fig.* 7. Plasma line spectra for 30 ms. heater pulses with 150 IPP at 7.3 MHz

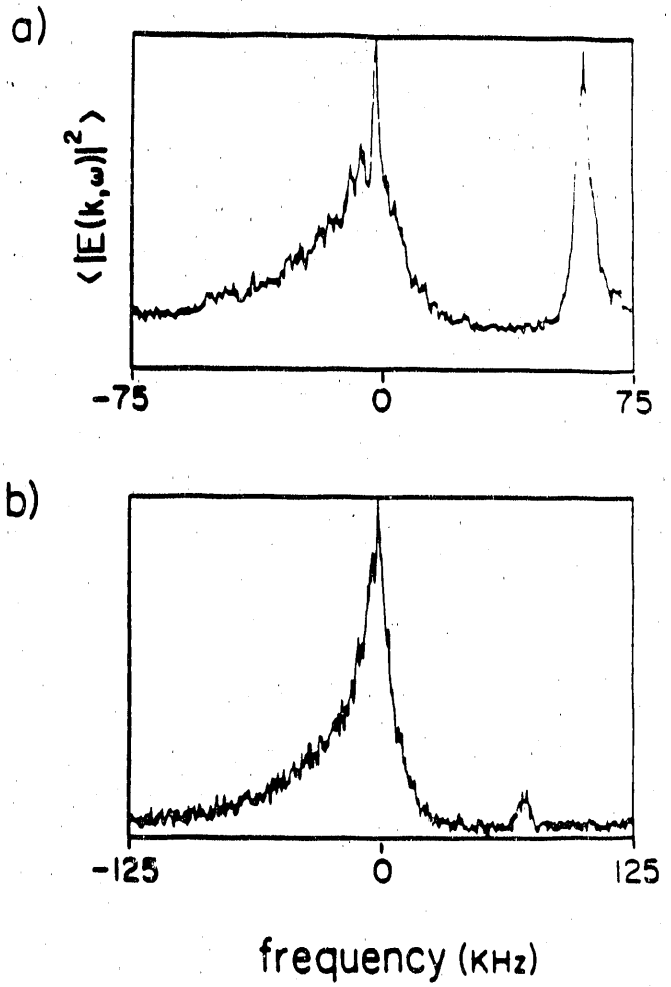


*Fig.* 6. Experimental spectra. (a) Heater pulse width 10 ms. IPP 150 ms. $f_H$ = 7.3 MHz spectra taken in 1.1 ms internals delayed 4 ms from onset of heating pulse. Note the free mode peak at ~72 kHz above the heater frequency which is 256 on the scale. (b) heater pulse width 10 ms. IPP 150 ms. $f_H$ = 7.3 MHz spectral delayed by 1.5 ms from onset of heating. Free mode peak at 52 kHz. From Cheung *et al.* [1989].

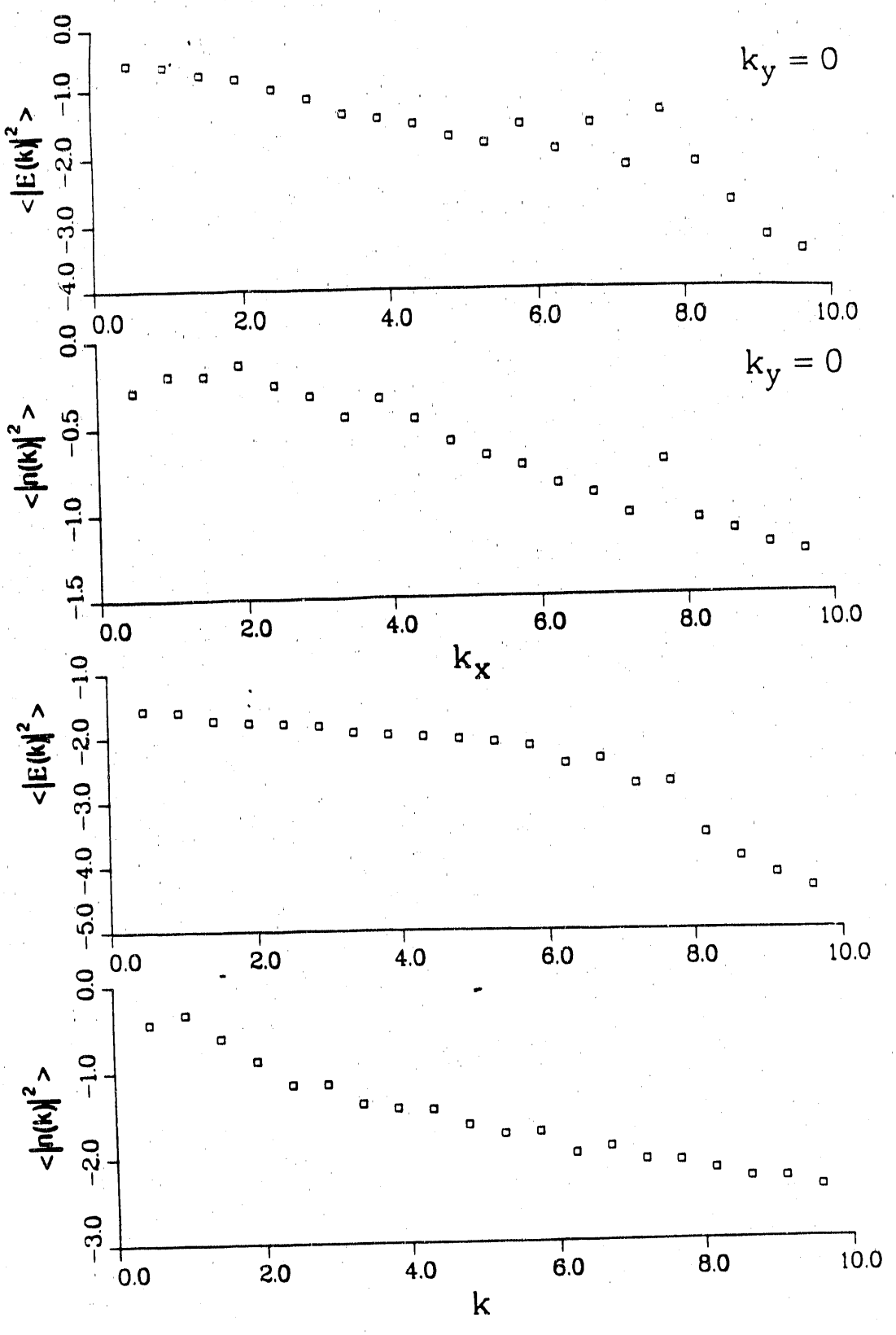


Fig. 8. Energy spectra $\langle |E(\underline{k}|^2 \rangle$ vs $k$ at $\theta$=0 (top panels) and $\theta = 60°$ for the parameters of Fig. 8 and with $Ly = 3^{-1/2} 2\pi k_*^{-1}$ and $Lx = 4\pi k_*^{-1}$ with (256×128) Fourier modes.

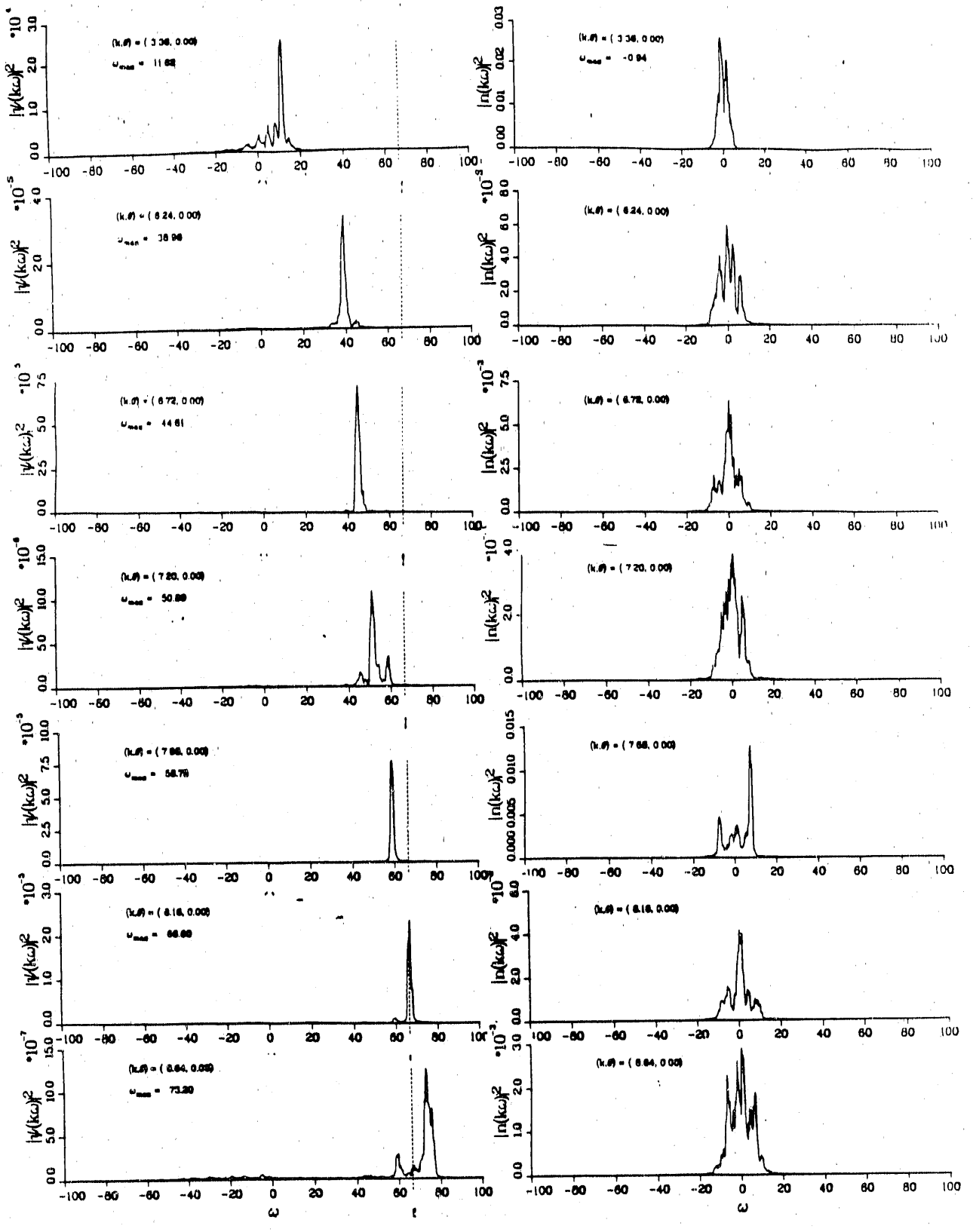

Fig. 9. Power spectra $|\psi(\underline{k},\omega)|^2 = k^{-2}\langle|\underline{E}(\underline{k},\omega)|^2\rangle$ (or plasma line spectra) on the left and $|n(\underline{k},\omega|^2$ (or ion line spectra) on the right for various values of k. For the parameters $E_o$=0.6, $\omega_o$ = 66.55, $\nu_i$ = 0.28, M=1836. In this case $k_i = 7.68, k_3 = 6.72, k_5 = 5.76, k_o = 8.16$ and $k_a = 8.64$.

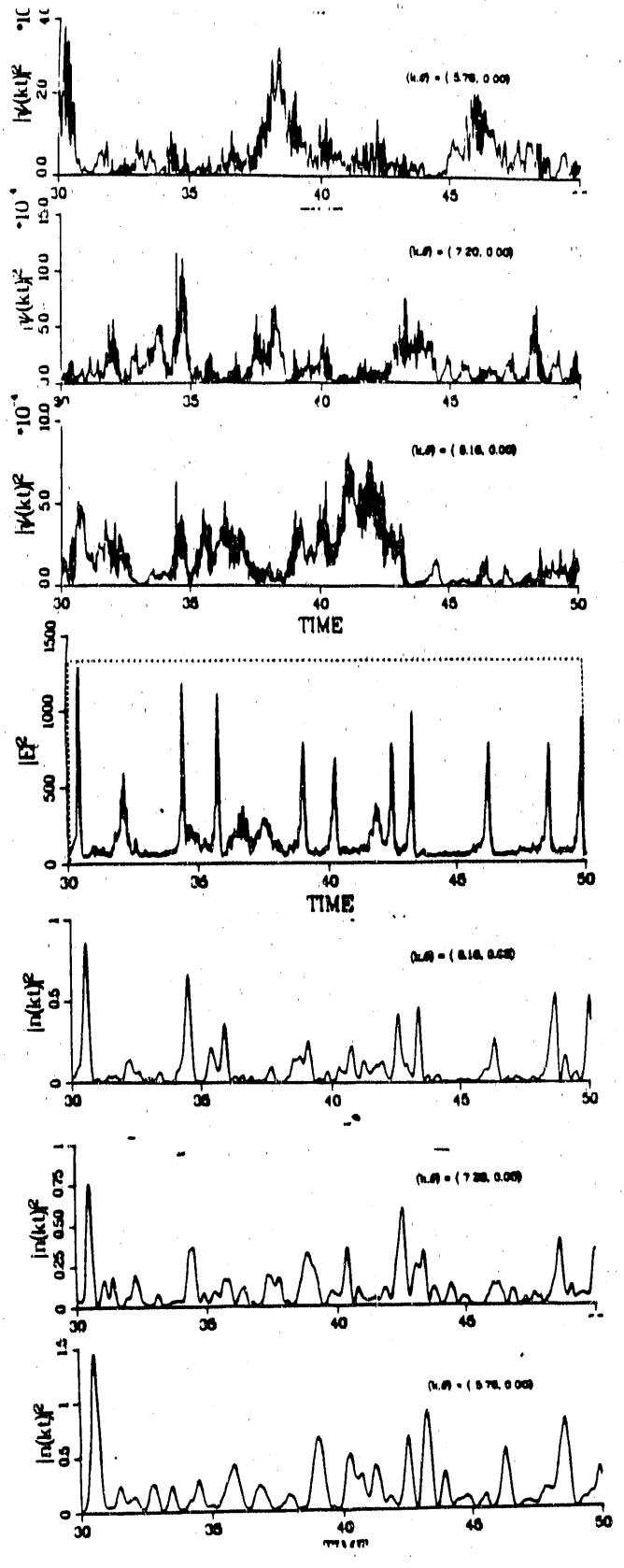


Fig. 10 Top three panels: Time history of Fourier modes $|\psi(k,t)|^2 = k^{-2}|E(k,t)|^2$ for various k values and the parameters of Fig. 8. Middle panel: $|E(x,t)|^2_{max}$ versus t; bottom three panels $|n(k,t)|^2$ versus t.

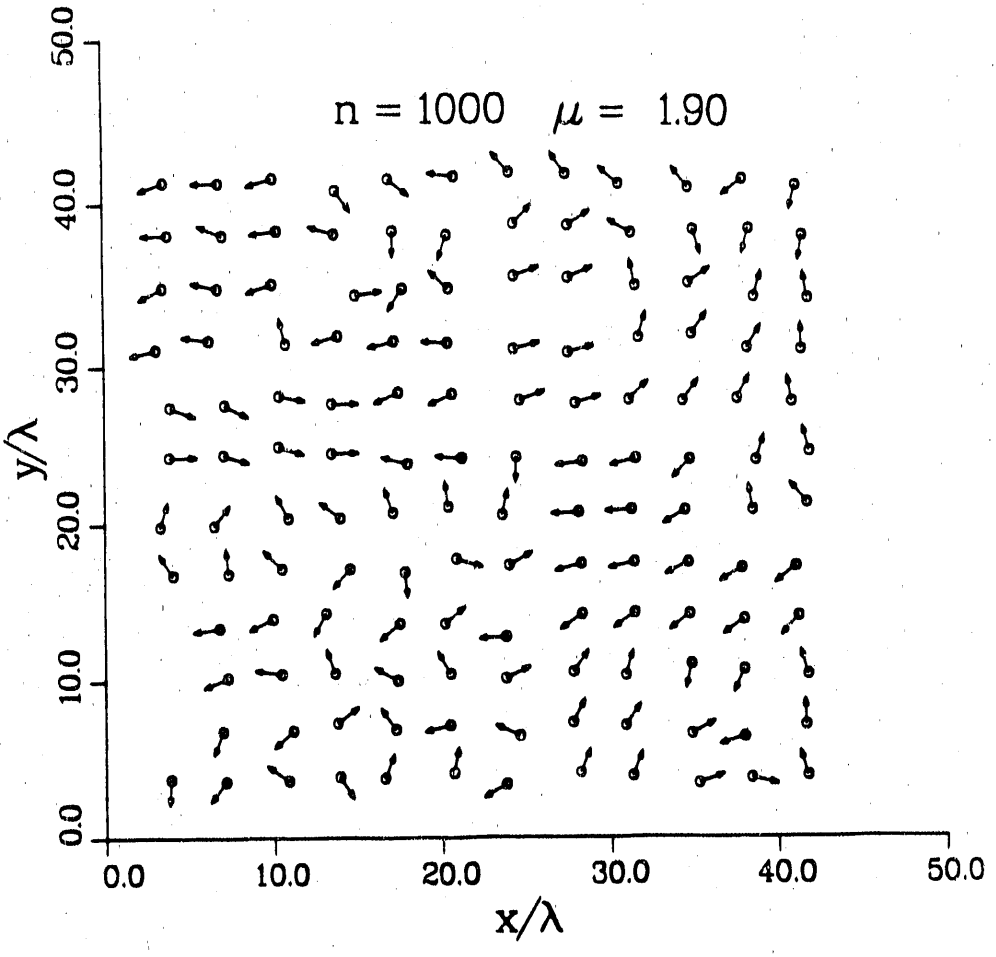


Fig. 11. illustrates the generation of collapse phase correlations between different cavitons in a multicaviton case. The initial state had no such correlations, but the cavitons were initially placed on a nearly regular square lattice. These correlations were strong after 10 collapses. Because the caviton motion is slow compared to its phase dynamics, 1000 collapses were followed to show that some degree of spatial regularity is retained after a time long enough such that spatial motion is significant. Note that the phase correlations are still strong even though the spatial distribution of cavitons is somewhat irregular. The direction of each arrow indicates the collapse phase at each site.

# END

# DATE FILMED

10/19/90